References and Notes

(1) Economy, J.; Volksen, W.; Viney, C.; Geiss, R.; Siemens, R.; Karis, T. *Macromolecules* **1988**, *21*, 2777.
(2) Mühlebach, A.; Lyerla, J.; Economy, J. *Macromolecules* **1989**, *22*, 3741.
(3) Karis, T.; Siemens, R.; Volksen, W.; Economy, J. *Mol. Cryst. Liq. Cryst.* **1988**, *157*, 567.
(4) Kricheldorf, H. R.; Schwarz, G. *Makromol. Chem.* **1983**, *184*, 475.
(5) Wunderlich, B.; Grebowicz, J. *Adv. Polym. Sci.* **1984**, *60/61*, 1. Hanna, S.; Windle, A. H. *Polymer* **1988**, *29*, 207.
(6) These annealing conditions were selected on the basis of data from Butzbach et al. (Butzbach, G. D.; Wendorff, J. H.; Zimmermann, H. J. *Polymer* **1986**, *27*, 1337) showing a maximum in the transition enthalpy of $T_{c\rightarrow n}$ for a 58/42 HBA/HNA random copolyester when annealed under these conditions.
(7) Mühlebach, A.; Johnson, R.; Lyerla, J.; Economy, J. *Macromolecules* **1988**, *21*, 3115.
(8) Windle, A. H.; Viney, C.; Golombok, R.; Donald, A. M.; Mitchell, G. R. *Faraday Discuss. Chem. Soc.* **1985**, *79*, 55.
(9) Annealing the sample IA at 205 °C for 24 h does produce a very small endotherm in the range of 245–260 °C. This small amount of transesterified product could arise from the presence of some very low molecular weight homopolyester(s) that melt (under the compression) and react. Very low molecular weight samples of poly(HBA) have been shown to enter a nematic melt under shear above the 340–350 °C transition. See ref 1.
(10) Economy, J.; Storm, R. S.; Matkovich, V. I.; Cottis, S. G.; Nowak, B. E. *J. Polym. Sci., Polym. Chem. Ed.* **1976**, *14*, 2207.
(11) If random copolyesters in the composition range 80/20 to 20/80 HBA/HNA are produced in the initial stages of the molding when the temperature is above 450 °C, they can continue to ester interchange to produce 50/50 random copolyester chains for ca. 400 s which is the time the mold remains above crystal to nematic transition temperatures for this entire range of copolyester composition.
(12) Jackson, W. J., Jr.; Kuhfuss, H. F. *J. Polym. Sci., Polym. Chem. Ed.* **1976**, *14*, 2043.
(13) Kugler, J.; Gilmer, J. W.; Wiswe, D. W.; Zachmann, H.-G.; Hahn, K.; Fischer, E. W. *Macromolecules* **1987**, *20*, 1116.
(14) Devaux, J.; Godard, P.; Mercier, J. P. *J. Polym. Sci., Polym. Phys. Ed.* **1982**, *20*, 1901.
(15) Ramjit, H. G.; Sedgwick, R. D. *J. Macromol. Sci., Chem.* **1976**, *A10*, 815.
(16) Kotliar, A. M. *J. Polym. Sci., Macromol. Rev.* **1981**, *16*, 367.
(17) Lenz, R. W.; Jin, J.-H.; Feichtinger, K. A. *Polymer* **1983**, *24*, 327.
(18) Economy, J.; Johnson, R. D.; Mühlebach, A.; Lyerla, J. *Polym. Prepr.* **1989**, *30* (No. 2), 505.
(19) De Meuse, M. T.; Jaffe, M. *Mol. Cryst. Liq. Cryst. Inc. Nonlin. Opt.* **1988**, *157*, 535.

Registry No. HBA (homopolymer), 30729-36-3; HBA (SRU), 26099-71-8; HNA (homopolymer), 94857-18-8; HNA (SRU), 87257-45-2; (HNA)(HBA) (copolymer), 81843-52-9.

Conformation of Comblike Liquid-Crystalline Macromolecules

Hedi Mattoussi*,† and Raymond Ober

Collége de France, Laboratoire de Physique de la matière condensée,‡ 11, place Marcellin Berthelot, 75231 Paris Cedex 05, France.

Received July 5, 1989; Revised Manuscript Received September 25, 1989

ABSTRACT: We have determined the conformation of side-chain liquid-crystalline polymers in nematic solutions by small-angle X-ray scattering. We have shown that the macromolecules are conformationally anisotropic. Moreover, the direction of anisotropy has been determined: the macromolecules are prolate ellipsoids ($R_{\parallel}\hat{n}_0 > R_{\perp}\hat{n}_0$), where $\hat{n}_0$ is the mean field nematic director. The form of the anisotropy and its magnitude appear to be independent of the coupling strength of the side groups to the backbone for relatively long spacers ($3 \leq n \leq 6$). The isotropic sizes R_i are large compared to an ordinary polymer with the same degree of polymerization. We have also measured the radius of gyration in an ordinary solvent (toluene) and found that the results are consistent with the nematic case. These results allowed us to point out an effect of the polymer concentration of the absolute sizes of polymer chains in ordered solutions but not on the form of the anisotropy or its magnitude. The results are consistent with an independent viscoelastic study reported on these materials and with the Brochard assumption that explains the typical nematic rotational viscosity behavior in these systems. We have compared these results with a recent theoretical approach by Warner et al.; there is a qualitative agreement between our results and the major points outlined in this model. Thus the correlation between mesomorphic order and anisotropy of chains is meaningful.

I. Introduction

The study of side-chain liquid-crystalline polymers has advanced considerably in recent years. The intense interest motivated by industrial applications has been stimulated by two factors: a wide variety of such materials has been designed by using advanced chemical reactions and new experimental and theoretical physical approaches have been made.[1-7] In fact these molecules have two conflicting properties: flexibility of the backbone, an aspect of conventional polymers, and nematic constraints due to the pendant groups that tend to orient the system because of the orientational order of mesomorphic materials.

Many structural studies of these systems in the melt phase have been reported, in either the smectic or the nematic state, depending on whether the investigated system shows one or more mesophases.[8-13] For instance, the arrangement of the side groups and that of the spac-

† Present address: Department of Chemistry, Carnegie Mellon University, 4400 Fifth Avenue, Pittsburgh, PA 15213.
‡ Unité associée au CNRS 0972.

0024-9297/90/2223-1809$02.50/0

ers between these groups and the backbone was examined by using NMR or X-ray diffraction.[12,13] The behavior of the skeleton has also been studied by using small- and wide-angle scattering techniques for various mesophases.[8-11] Other studies such as dielectric relaxation,[14] storage devices,[15] defects approach as for conventional liquid crystals,[16] and structural investigations by infrared spectroscopy[17] have been reported on these materials.

The study of these systems in solution, mainly in nematic solvents, is still incomplete. One might be able to draw an analogy with ordinary solutions of flexible polymers. Mesomorphic solutions have the advantage of being able to orient; thus the classic liquid crystal physical approaches can be used. Another advantage of solution study is that it allows one to gain access to compounds that are sometimes impossible to handle in melt phase.[18]

We pursued a viscoelastic study of side-chain polysiloxane in a low molecular weight (lmw) liquid crystal solvent. We measured the typical nematic rotational viscosity γ_1 as well as the Frank elastic constants.[18,19] This method is used to check the effect of dissolved macromolecules on the properties of liquid crystals. However, it has also provided us with information concerning the behavior of solute chains in such a mesophase order. In particular, the explanation for the viscosity increase, in terms of the hydrodynamic model of F. Brochard,[20] points to a conformational anisotropy of the macromolecules. This hypothesis is also useful in interpreting other similar studies in melt systems.[4,21] However, the viscoelastic study coupled with the anisotropy hypothesis do not enable us to determine the shape (prolate, oblate, etc.) of the macromolecules.

We reported in a previous communication[22] a preliminary small-angle X-ray scattering study (SAXS) carried out on such macromolecules in a nematic solvent. In the present report we present a wide ranging study with more detailed results taking into account the different parameters involved in these systems such as the effect of concentration and the phase state. We also report complimentary study in an ordinary solvent to check these results. This has allowed us to make a better correlation with the viscoelastic study. The results were interpreted qualitatively in the framework of the phenomenological model of Warner et al.[23]

II. Experimental Section

1. Materials and Sample Preparation. We used the poly(methylsiloxane) side-chain polymers, extensively described in previous works.[19,22] They were synthesized by H. Finkelmann (W. Germany), by substitution of phenyl benzoate liquid crystal groups on a given poly(methylsiloxane) chain. During the chemical reaction, each H atom previously linked to Si is replaced by a nematic molecule that is attached to the backbone through a methylene chain $(CH_2)_n$, called the spacer (n). The polymers are symbolized by P_n^N, where N and n are the degree of polymerization and the spacer length, respectively. We used systems with N values of 95 and 50 and varied n between 3 and 6. The nematic solvent (symbolized by M_2) was a phenyl benzoate liquid crystal very similar to the mesomorphic side groups. The corresponding clearing temperatures are listed in Table I.

M_2 and P_n^N were determined to be compatible before any measurements were made. The close chemical similarity between the solvent molecules and the pendant groups does not guarantee miscibility. In fact, recent studies of Casagrande et al. and Siguad et al.[4] have shown that the phase separation process is sensitive to small modifications in the aliphatic chains as well as to the nature of the hard core of the nematic molecules.

Table I
Chemical Formulae and Clearing Temperatures for Polymers P_n^N and lmw Liquid Crystal Solvents Used

material		T_c, K
$C_6H_{13}OPhCOOPhOC_2H_5$	M_2	367.3
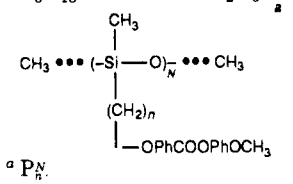	P_3^{95}	356–357.8
	P_4^{95}	376–376.5
	P_5^{95}	390.8–392
	P_6^{95}	385–385.3
	P_6^{50}	379–380.1

[a] P_n^N.

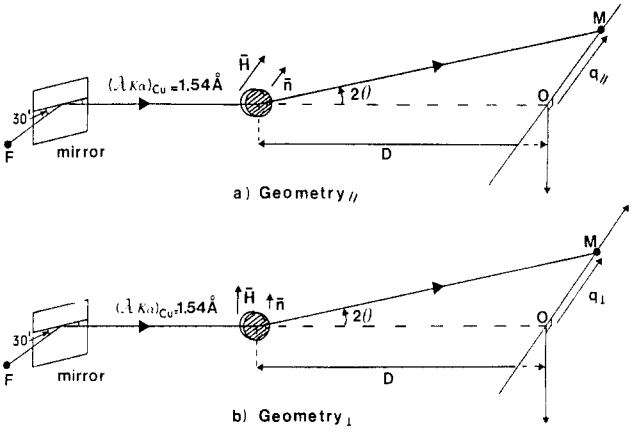

Figure 1. Experimental setup.

We prepared nematic solutions of about 4–5 wt % by carefully agitating the $P_n^N + M_2$ mixture in vacuum-sealed tubes at a temperature slightly above the clearing point. The cells for X-ray measurements were flat cylinders with a diameter of 5 mm, a 1.5 mm optical path, and mica windows 25 ± 2 μm thick. Only one concentration of each solute was used. In fact, the number of samples was limited by the impossibility of reconditioning used solution and the large volume of material required for each cell. [The special conditions in which the samples are used (high temperatures, the need for a monocrystal, ...) made it very difficult to retrieve a solution without contaminating it or damaging the cell.] In addition, the relatively weak contrast of solute macromolecules limited our ability to use smaller concentrations.

As an ordinary solvent, we used toluene which has the closest electron density to the phenyl benzoate solvent; it is also a good solvent for the polymer. Capillary tubes of 1 mm diameter were used as sample holders for X-ray measurements. In this case, the higher electronic contrast and the possibility of reconditioning the solutions allowed us to explore many values of polymer concentrations.

2. Experimental Setup. The experimental setup is shown schematically in Figure 1. The distinction between the two geometries ∥ and ⊥ is made only for mesophase-ordered solutions. For isotropic phases and conventional solutions these geometries were identical. The X-ray generator source was a rotating copper anode machine (RIGAKU) operated at 40 kV and 20 mA. The apparent source irradiates an area of 10^{-2} mm^2. Because of its property as a total reflector for the copper wavelengths $\lambda_{k\alpha)Cu}$ and $\lambda_{k\beta)Cu}$, a vertical mirror, composed of a gold deposit on a quartz surface, was used to eliminate the short wavelengths and to focus the X-ray beam on the position-sensitive detector (PSPE) (ELPHYSE). The wavelength $\lambda_{k\beta)Cu}$ was then altered by a nickel filter.[24]

The incident beam had a vertical rectangular shape, 3 mm × 0.3 mm in dimension. The detector had a 3 mm window, a useful length of 50 mm, and 200 μm spatial resolution. The distance D was 500 mm.

The nematic samples were placed in an oven designed to have an accurate temperature control ($\Delta T < 0.2$ °C) and to allow the X-ray beam to pass through.[18] The samples were subjected to a permanent magnetic field ($H \simeq 1.4$ kG) to ensure homogenous liquid-crystalline order. H could be oriented either

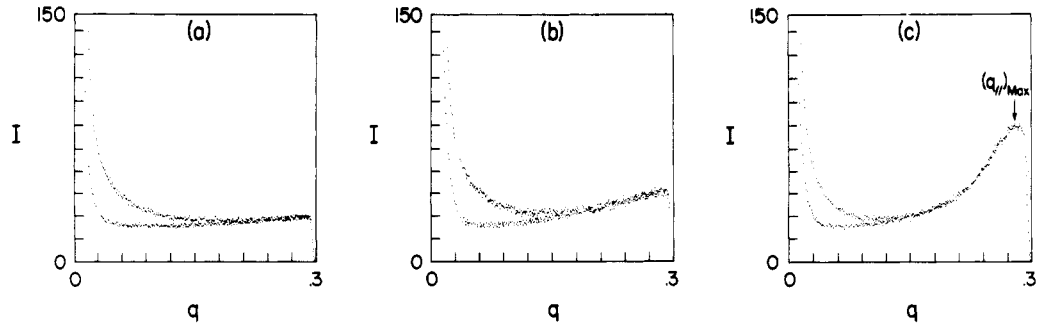

Figure 2. Crude spectra: (a) nematic state, geometry $\perp$; (b) isotropic state ($P_n^N + M_2$); (c) nematic state, geometry $\parallel$.

horizontally or vertically with respect to the detector. In each case a scattered intensity either parallel ($q_\parallel$) or perpendicular ($q_\perp$) to the nematic direction ($\vec{n}_0$) was allowed.

For each system we proceeded in the same way. The scattered useful intensity was obtained from the difference spectrum between the solution and the reference (pure solvent) after making the required correction for the attenuation due to passage through the sample and the counting time.

3. Small-Angle Spectra and Method of Analysis. We recall that for the general case, the scattered X-ray intensity normalized to the electron scattering intensity I_e may be expressed as[29]

$$I(q,c) = KcM(S(q)\chi_T(q)) \tag{1}$$

where c is the concentration (g/cm^3), M is the molecular weight of the macromolecule, K is the experimental constant depending on the electronic contrast $(\Delta\rho)^2$ and the Avogadro number N_A [$K \propto (\Delta\rho)^2(1/N_A)$], $S(q)$ is the single chain contribution or form factor, and $\chi_T(q)$ is the interaction contribution or structure factor. $\chi_T(q)$ is related to the virial coefficient.

For the conditions $c \ll 1$ and small q values (Guinier limit $qR < 1$) $I(q,c)$ can be written as

$$\frac{KcM}{I(q,c)} = S^{-1}(q)\chi_T^{-1}(q) \approx 1 + q^2\frac{R_G^2}{3} + 2A_2Mc + \dots \tag{2}$$

R_G is the radius of gyration defined by

$$R_G^2 = \frac{1}{2N}\sum_{i,j}\langle (r_{ij})^2\rangle \tag{3}$$

where the summation is taken over all monomers i and j in the chain and r_{ij} designates the distance between these monomers; N is the degree of polymerization. A_2 is the second virial coefficient.

For finite and small q and c values, this expression plotted in a double diagram c/I vs $(q^2 + c)$ (Zimm plot) provides R_G and A_2, respectively, at the limits $c = 0$ and $q = 0$.

For only one finite concentration eq 3 reads

$$\frac{KcM}{I(q,c)} \approx \frac{KcM}{I(0,c)}\left(1 + q^2\frac{R_G^2}{3}(c) + \dots\right) \tag{4}$$

Therefore, a plot of I^{-1} vs q^2 can provide us only with an apparent radius of gyration taking into account interactions between chains in the solution. In the present study, we were able to extract R_G from Zimm plots of ordinary solutions. For the nematic solutions, however, we extracted only apparent dimensions.

For the liquid crystal solutions in the nematic phase, the system possesses a uniaxial symmetry and consequently $S(q)$ does also. This may be deduced from the corresponding scattered intensity parallel and perpendicular to the nematic $\vec{n}_0$.

We define two characteristic dimensions for the macromolecules[22,26]

$$R_\parallel^2 = \frac{3}{2N}\sum_{i,j}\langle (r_{ij})_\parallel^2\rangle \tag{5}$$

$$R_\perp^2 = \frac{3}{2N}\sum_{i,j}\langle (r_{ij})_\perp^2\rangle \tag{6}$$

where $(r_{ij})_\parallel$ and $(r_{ij})_\perp$ are respectively the projections of $\vec{r}_{ij}$ on the axis parallel and perpendicular to $\vec{n}_0$. This definition involves the uniaxial symmetry property and verifies

$$R_\parallel^2 + 2R_\perp^2 = 3R_G^2 \tag{7}$$

In the Guinier approximation ($qR_{\parallel,\perp} < 1$) the scattered intensities (eq 4) may be expressed as

$$I_\parallel^{-1}(q,c) = I_\parallel^{-1}(0)\left(1 + q^2\frac{R_\parallel^2}{3}(c)\right) \tag{8}$$

$$I_\perp^{-1}(q,c) = I_\perp^{-1}(0)\left(1 + q^2\frac{R_\perp^2}{3}(c)\right) \tag{9}$$

These expressions are equivalent in the isotropic phase and read

$$I_i^{-1}(q,c) = I_i^{-1}(0)\left(1 + q^2\frac{R_i^2}{3}(c)\right) \tag{10}$$

Consequently, one can extract the following: two sizes, $R_\parallel$ and $R_\perp$, for the nematic state and the dimension R_i for the isotropic state from the plots of $I^{-1}{}_{\parallel,\perp,i}(q)$ vs q^2, respectively [all three of these parameters are concentration dependent and consequently are only apparent values; we could not have access to A_2 in this case since we were not able to scan different concentrations, particularly small values of c (see above)]; R_G and A_2 for the ordinary solutions, from the Zimm plots.

We will show subsequently that the two series of measurements are very consistent and give complimentary information.

Remark: Although the similarity of chemical structure of the two solvents (M_2 and toluene), there is a difference in the effective chain contrast. On the basis of these considerations, in principle one would extract signals due to the backbone from nematic solutions. However, the signal will arise from the whole chain, including side groups for the case of ordinary solutions.

III. Results

1. Scattered Spectra. The crude spectra for ordinary solutions show ordinary behavior with a large contribution from the solute chains at the small scattering vector limit and a continum decay to zero for high q values and consequently do not need to be considered. However, a detailed analysis of these spectra is of interest in the nematic case.

Parts a–c of Figure 2 show three spectra corresponding to the two geometries for the nematic phase and the isotropic phase. The contribution from the macromolecules is limited to low q values in all cases. Conversely for wide angle measurements, the shape of the spectra reflects the characteristics of each case. The intensity peaks at wide angles registered for the sample and the reference in the parallel geometry reflect the liquid crystal correlations in the direction parallel to the nematic

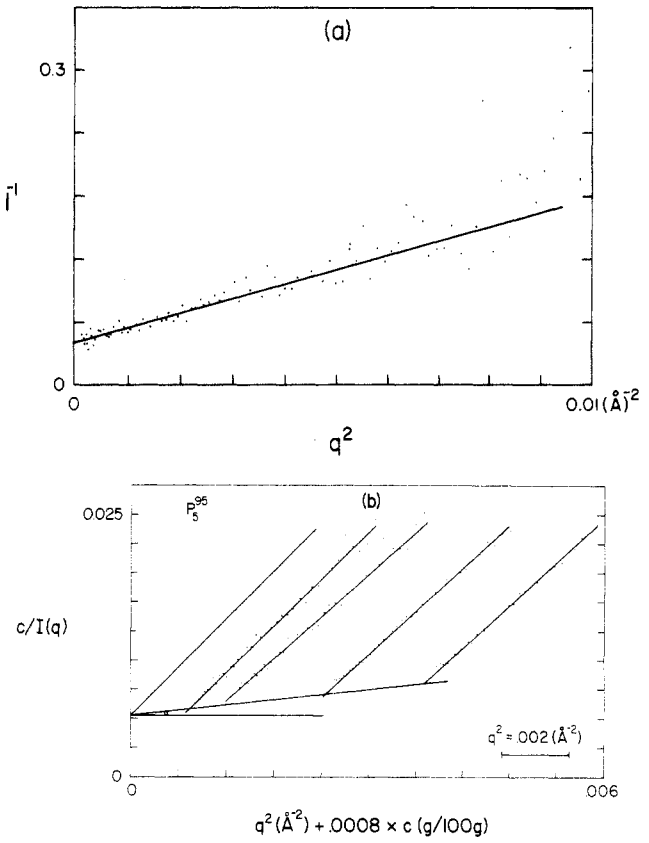

Figure 3. I^{-1} vs q^2 spectra: (a) typical small-angle difference spectrum; (b) typical Zimm plot for solutions in toluene.

director $\vec{n}_0$. In fact, the dimension l deduced from this position, $(q_\parallel)_{max} = 0.28$ Å^{-1}, is of the order $l = 2\pi/(q)_{max} = 22$ Å, a value typically characteristic of lmw mesomorphic molecules. It is also interesting to note that the peak intensities are similar for the nematic solutions and the pure solvent. This reflects the fact that the peaks arise mainly from the liquid crystal part contribution. For the perpendicular case the peaks will be shifted to higher q values $[(q_\perp)_{max} \gg (q_\parallel)_{max}]$, since they arise from correlations transverse to the nematic direction. The isotropic case is intermediate between those described above (Figure 2b). The absence of order gives a contribution intermediate between the ($\parallel$) and ($\perp$) cases.

Finally, it is important to note the net distinction between the two contributions (from macromolecules and liquid crystal molecules). This property is crucial since our aim is the extraction of signal due to the chains. The above distinction ensures that the signal studied at low angles is essentially due to solute chains: $q < 0.18$ Å^{-1}.

2. Small-Angle Intensity Spectra. Figure 3 shows a typical I^{-1} vs q^2 plot for a solution $P_n^N + M_2$ and a linear increase for the small q limit is easily observed. The scatter in the experimental data for higher angles is mainly due to the poor signal to noise ratio where the difference in intensity between the solution and the reference approaches zero. Similarly, a typical Zimm plot is shown in Figure 3b for P_n^N in toluene solutions; the set I^{-1} vs q^2 are also linear in this case. We note that the analysis is limited to small q values to ensure that the two following requirements are satisfied: being in the Guinier zone and avoiding the lmw nematic contribution.

3. Characteristic Sizes and Conformational Anisotropy. Table II presents the characteristic dimensions $R_\parallel$ and $R_\perp$ of the nematic state (N) and R_i of the isotropic phase (I) for the mesomorphic solutions. The principal results of these measurements may be split into four parts:

(a) The macromolecules sizes in the directions $\parallel$ and $\perp$ to the mean field director (n_0) are *effectively different*. Hence, the hypothesis of conformational anisotropy in ordered media (N) is useful for understanding these systems. Moreover, the present measurements complete that hypothesis by providing the form of the anisotropy and its magnitude:

$$R_\parallel > R_\perp \text{ and } R_\parallel/R_\perp \approx 1.3 - 1.6 \qquad (11)$$

The difference between these two sizes is larger than the experimental uncertainties.[36]

(b) The characteristic sizes $R_\parallel$ and $R_\perp$ in the phase (N) do not evolve in a strong temperature-dependent manner except within a range close engough to the clearing point.[18,22] The magnitude of the anisotropy is also very weakly dependent on the spacer length, for $P_n^N + M_2$ systems (Figure 4).

(c) The chain dimensions in the disordered phase (state I), R_i, are large compared to conventional chains with a similar degree of polymerization. For instance, a poly(dimethylsiloxane) chain (PDMS) Gaussian coil, with $N \approx 100$ and a statistical element of $b \approx 5.4$ Å,[27a] would give $R_G \approx 18.5$ Å to be compared to $R_i \approx 45$ Å for P_3^{95} at $c \approx 5.5\%$ (w/w). The measured dimensions for the nematic solutions are consistent; they obey the volume conservation condition (eq 7) and $R_\perp < R_i < R_\parallel$ (Figure 4).

(d) For ordinary solutions (in toluene), the values of $R_G(c = 5\%)$ and $R_G(c = 0)$ as well as the virial coefficients A_2 extracted from Zimm plots are reported in Table II and Figure 5. We effectively determined an apparent radius of gyration for finite concentration ($c \neq 0$), with $R_G(c \neq 0) < R_G(c = 0)$. For P_6^{95} and P_6^{50}, we have determined that $R_G(P_6^{50}) < R_G(P_6^{95})$ and that the corresponding ratio is about $(95/50)^{1/2}$.

IV. Discussion

1. Comparison between the Two Systems. The measurements in toluene complement those in the lmw nematic solvent: For comparable concentration values, the dimensions R_i and R_G are very close; for example $R_i \simeq R_G \simeq 45$ Å for P_3^{95} and at $c \approx 5\%$. For finite c values the apparent radius of gyration $R_G(c)$ is determined. The virial coefficients deduced above (Table II) are in good agreement with theoretical estimations deduced from a spheres model (M = coil mass):[28]

$$A_2 = 4/3(\pi R_G^3/6M^2) \qquad (12)$$

This agreement clearly shows the compensation effect between the large size measured and the relatively high molecular weights of the PMS side groups used:[37] for $N \approx 100$, M(PDMS) ≈ 7000 and M(PMS) $\approx 34\,000$.

On the basis of these results, one can explain the fluctuations in absolute sizes from one compound to another in nematic solutions as a concentration effect. In fact due to the similar values of R_i and R_G for similar concentrations one can assume that A_2 is also positive in nematic solutions. We have checked that the evolution of $R_{\parallel,\perp,i}$ is consistent with this assumption as c varies from one solution to another: The sizes increase when c decreases.

Another interesting point that comes out of this comparison is that the difference in contrast between the two solutions does not affect the overall size determination significantly.

We also tried to deduce a persistence length for these systems since the knowledge of this parameter could give

Table II
Characteristic Dimensions: (a) $R_\parallel$, $R_\perp$, R_i, $R_\parallel/R_\perp$, and R_G at $c \approx 4$–5% for P_n^N Components and (b) $R_G(c=0)$ and A_2 for P_n^N Solutions in Toluene

	P_3^{95}	P_4^{95}	P_5^{95}	P_6^{95}	P_6^{50}
R_G(5%) in toluene, Å	46	47	47.5	50	43.5
R_{iso}, Å	45.5	55	58	45	
$R_\parallel$(80 °C), Å	53		75	68	
$R_\perp$(80 °C), Å	34		53	45	
$R_\parallel/R_\perp$(80 °C), Å	1.56		1.41	1.51	
$R_\parallel$(85 °C), Å	52	67	73	64	
$R_\perp$(85 °C), Å	35	44	54	45	
$R_\parallel/R_\perp$(85 °C)	1.48	1.52	1.35	1.42	
A_2, cm^3/g^{-2}	1.8×10^{-4}	1.60×10^{-4}	1.70×10^{-4}	2.70×10^{-4}	2.40×10^{-4}
A_2(theo) $= (4/3)R_G^3/6M^2$	1.25×10^{-4}	1.04×10^{-4}	1.1×10^{-4}	1.85×10^{-4}	2.93×10^{-4}
$R_G(c=0)$, Å	57	55	57.50	70	50.5

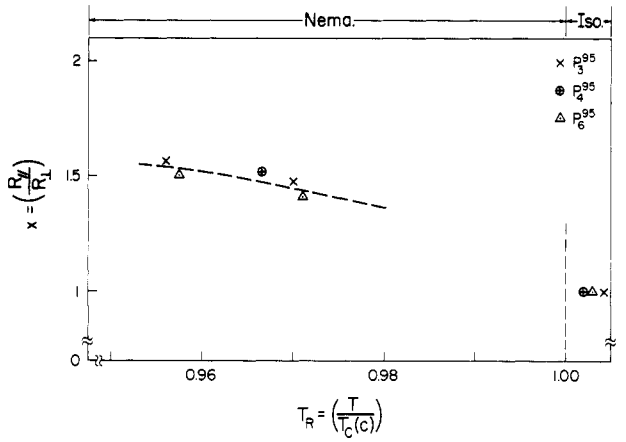

Figure 4. Evolution of ($x = R_\parallel/R_\perp$) with reduced temperature T_R.

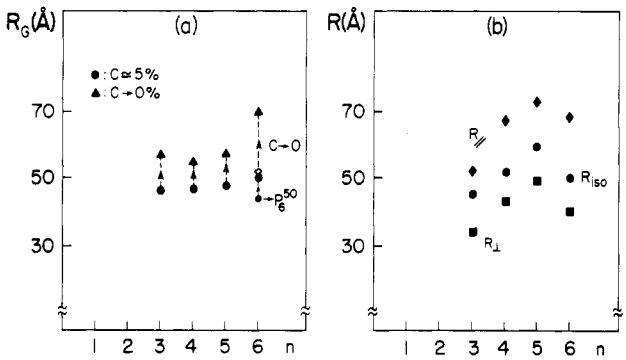

Figure 5. Evolution of the macromolecule dimensions with the spacer value: (a) $R_G(c)$ for c varying from 5% to 0, for P_n^N; (b) $R_\parallel$, $R_\perp$, and R_i for different P_n^N.

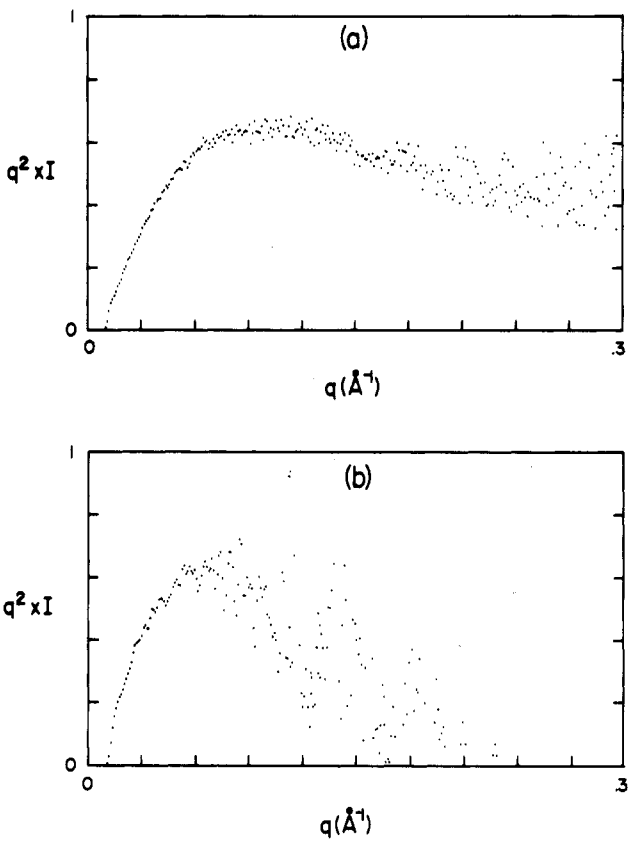

Figure 6. Typical Kratky plot for solutions: (a) in toluene; (b) in the nematic solvent M_2.

a better insight into the understanding of the global chain behavior. Figure 6 shows a Kratky plot of $q^2I(q)$ vs q for both solution systems. The two curves are similar with a decreasing curve at high q vectors. The large scatter in the experimental data, mainly for the ($P_n^N + M_2$) case, is due to the low signal to noise ratio in that q range. No persistence length could be deduced from these curves since they deviate from the classical linearly increasing curves for ordinary polymers.[29] This phenomena can be explained by taking into account the side group effects. In fact for macromolecules with a transverse extension there is a second contribution to the scattered intensity arising from the side group correlations which, in the framework of a cylinder chain of radius R_c, would read as

$$\Psi(q) \simeq \exp(-q^2R_c^2/2) \quad (13)$$

The total scattered intensity for one chain will then read

$$J(q) = S(q)\Psi(q) \quad (14)$$

The Kratky curve $q^2J(q)$ vs q will decrease at high angles. The larger the cross-sectional radius is, the sharper the decrease in that curve for the high q range will be. If we assume $R_c \simeq 20$ Å, for the side group size, the exponential term reaches already e^{-1} for $q = (2)^{1/2}/20 = 0.07$ Å^{-1}. These observations are consistent with previous neutron or X-ray scattering studies of ordinary polymers with partial side-chain extension.[30,31]

One can summarize the overall effects of mesomorphic pendant groups on the physical properties of these systems in two ways: First is the size of the macromolecules: the presence of nematic groups causes a larger radius of gyration compared to conventional chains regardless of the type of solvent used. Similar results have been mentioned recently for side-chain polymethacrylate liquid crystal.[27b] Second is the anisotropy of conformation in an ordered state medium; the effect of the polymerization index could not be systematically checked. (We

Table III
$R_\parallel$, $R_\perp$, and $R_\perp/R_\parallel$ for Other Structural Measurements[8-10]

component	M_w	N_w	$R_\parallel$, Å	$R_\perp$, Å	$R_\perp/R_\parallel$	R_{iso}
PMA[8]	425.000	1020	94 ± 5	118 ± 6	1.25	108
PMA[9]	300.000	660	102 ± 8	112.6 ± 8	1.10	106
PMA[10]	≪300.000	≪660	45	49.5	1.07	≃50
PMS[10]	15.000	≃35	~33	25	0.75	≃29

could not extract any meaningful results from $P_6^{50} + M_2$ solutions.)

2. Comparison with Other Results. First, it is interesting to compare these results to viscoelastic studies. The anisotropy of conformation proves the validity of the hypothesis with which we have explained our viscosity measurements.[18,19] This study complements that hypothesis since it allows us to determine the form of the anisotropy in such systems. Another important point is that the radius of gyration measured in ordinary solutions provides us with values of the overlap concentration c^*. These values coincide well with the crossover region for viscosity behavior.[18,19]

The comparison with other similar measurements, even though it is useful, must still remain partially incomplete, since at least one major component of the system varies in each comparison: mesomorphic state, nature of the backbone, phase of the system (melt or solution), and chemical properties of the side-chain macromolecules.

Early work by Dubault et al.[26] using a nematic solution of short polystyrene chains reported a very weak anisotropy: $R_\parallel \simeq 27$ Å and $R_\perp \simeq 22$ Å ($\Delta R_{\parallel\perp} \approx 4$ Å). This result is not surprising when compared to NMR results.[26] In fact the chains show local order (due to the nematic arrangement), but the global anisotropy is sensitive to the size of the chains and hence is difficult to observe for the chosen small molecular weight (PS = 2100). Given these reservations, there is, however, a slight tendency toward a prolate form in this case.

All other measurements have been made on similar side-chain polymers by using small-angle neutron scattering on labeled melts. We have summarized these results in Table III: Kirste et al.,[8] Keller et al.,[9] and Moussa et al.,[10] have used the polymethacrylate side-chain components. The pendant groups vary from one study to another, yet the results agree for the direction of the anisotropy with oblate chains; however, the magnitude of anisotropy varies from one component to another depending on the molecular weight and the nature of the terminal groups in the nematic parts. More, this magnitude is strongly dependent on the mesomorphic state if more than one phase exist. On the other hand, Moussa et al.[10] and Kunchenko et al.[11] used poly(methylsiloxane) backbones with different degrees of polymerization as well as different pendant groups. For relatively short chains ($N \approx 35$), it was found that the chains have a prolate form[10] in both smectic and nematic states. The chains have an oblate form in the smectic phase for relatively a high polymerization index ($N \approx 65$) and with strongly polar side groups.

All these results show that many factors influence the direction of anisotropy as well as its magnitude: backbone flexibility, the nature of the nematic side groups, mesomorphic state, coupling strength between the backbone and liquid crystal groups (spacer length), etc. Comparisons of all these results cannot be conclusive, since the authors did not use similar systems in the same physical state. On the other hand, comparison with the present case is even more difficult since the systems studied are basically different. A difference in physical behavior between melts and solutions is common. One can recall that excluded volume effects are only a property of solutions. A similar example for nematic polymers is worth mentioning; it has been observed that starting from a negative optical anisotropy, $\Delta n = n_e - n_0 < 0$, for very short spacers in the melt phase, one can end up with a positive value for even a slight dilution in lmw liquid crystals ($c = 95\%$).[32]

The wide variety of experimental results for these systems seem difficult to understand a priori; however, a theoretical approach was recently developed by Warner et al. This approach provides an insight into the understanding of these problems and qualitative explanation for the variety of anisotropic forms. The model was initially developed for melt systems, but the principal tools might be of use in interpreting the results of the present study.

3. Comparison to the Model of Warner et al. We first outline the major tools used in this approach. The original idea was developed by Warner et al.[33a] for main-chain liquid-crystalline polymers. It consists of analyzing the evolution of the unit vector tangent to the trajectory of a polymer chain. This vector $\vec{u} = \vec{u}(s)$, where s is the curvilinear abscissa, defines the local angle θ between the trajectory of the chain and the main field nematic orientation $\vec{n}_0$. Two interaction parameters were introduced: a bending term ϵ and a mean field liquid crystal term a (Maier–Saupe interactions, MS).[34] The evolution of $\vec{u}$ along the chain is equivalent to a displacement on the surface of a sphere with a unit radius, while keeping perpendicular to that surface. θ is the angle characterizing the relative direction of $\vec{u}$ compared to the z axis ($\parallel \vec{n}_0$). This is similar to the model developed by Debye to analyze the orientational diffusion of rigid rods in solutions.[35] The principal physical parameter derived from this model is a potential barrier W (similar to that for a flying quantum particle), expressed as

$$W = -3aS\beta^2\epsilon = -\frac{3aS\beta}{2D} \qquad (15)$$

where D is an angular diffusion coefficient on the sphere surface, a is the MS interaction parameter, S is the mean field order parameter, and β is the inverse of the Boltzmann factor. $W < 0$ corresponds to a vector confined to the polar regions of the sphere; there is a repulsion W on the equator. This will correspond to a stretched chain in the nematic state which seems to be a common feature for these systems. The condition $R_\parallel/R_\perp > 1$ is always present. The magnitude of the anisotropy depends on $|W|$.

This idea has been generalized by Wang and Warner to comblike polymers.[33b] To account for the different elements in the chain, these authors have introduced several interaction parameters (Figure 7) and two order parameters, S_B (backbone) and S_A (nematic groups). This model includes the case where there are nematic elements in the backbone. In accordance with the same major features mentioned above, a new expression depending on these parameters is derived for the potential barrier W

$$W = -\frac{3\beta}{2Dl}((1-\phi)v_B S_B + (\phi v_c - v_f/n)S_A) \qquad (16)$$

$$W \propto \epsilon$$

where ϕ denotes the fraction of side groups compared to the whole macromolecule, n is the spacer, and l is the cross section of the backbone. The most striking point of this expression is that it includes the two conditions $W > 0$ and $W < 0$. $W < 0$ corresponds to the previous

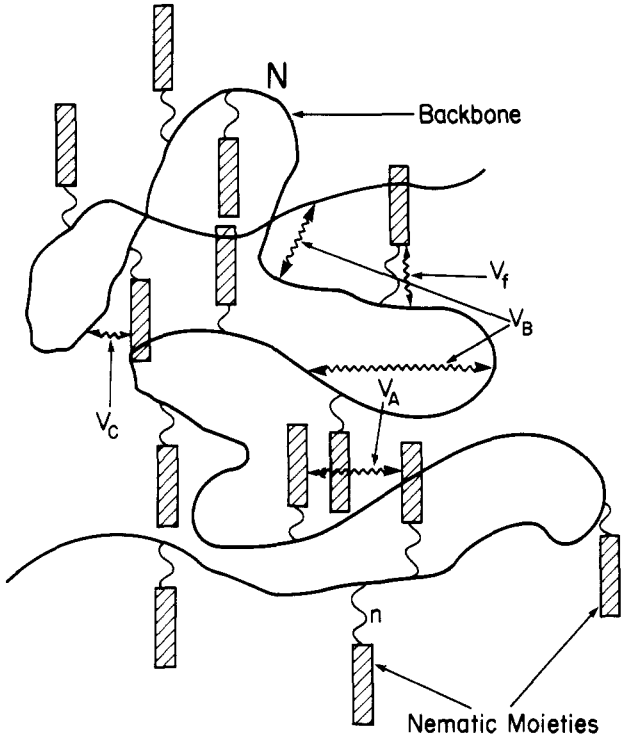

Figure 7. Schematic representation for interaction parameters (v_A, v_B, v_C, v_f) introduced by Warner et al.

case, and a prolate chain can exist. At the opposite case, the chains are flattened (oblate) for $W > 0$ and the vector $\vec{u}$ is limited to the equatorial region, on the unit sphere introduced above.

Let us discuss some physical aspects of this formulation with comparison to the different systems studied so far. The parameter W is proportional to ϵ. For *flexible* backbones such as PMA or PMS, ϵ is *small* and hence $|W|$ is also small. This produces a three-dimensional conformational extension in both the prolate and oblate cases. This feature is quite consistent with the relative values for $R_\parallel$ and $R_\perp$ for these systems (Table III). The flexibility of these backbones might give rise to zero values of S_B and v_B. The expression above turns out to be

$$W = -\frac{3\beta}{2Dl}(\phi v_c - v_f/n)S_A \qquad (17)$$

The form of the anisotropy will depend on the relative importance of the terms ϕv_c and v_f/n. For instance, the inequality $\phi v_c > v_f/n$ corresponds to a prolate chain. This might be the case for cumbersome side groups with long spacer and the case where these groups are sufficiently decoupled from the backbone.[38] The case of relatively short nematic portions, frequent pendant groups along the backbone, and a strong coupling through the spacer elements would correspond to the opposite figure with $\phi v_c < v_f/n$. The first case could be suitable for the PMS case and the second for the PMA case.

These considerations remain valid for solutions. The change from considering systems in the melt state to solution may be accompanied by a relative modification of the parameters used. In fact the influence of nematic elements is more important even if they are not all directly connected to the backbone. This argument could be translated into a fairly weak first term in eq 16 ($1 - \phi \simeq 0$), as mentioned above, but most likely to a predominance of the ϕv_c term in eq 17. This property could lead to a negative potential barrier for solutions, even if we start with the positive case in the melt phase. Therefore the chains will have more facility to organize in a prolate form. This may be checked if one studies solutions of other side-chain polymer systems by neutron scattering, for instance.

Conclusion

We have reported a conformational study of side-chain poly(methylsiloxane) liquid-crystalline polymers, in a lmw mesomorphic and ordinary solvents, by small-angle X-ray scattering. The main result presented is that the backbone has an anisotropic conformation in ordered media. This feature is consistent with the Brochard hypothesis used to interpret previous viscoelastic studies. Moreover, the present measurements complement this hypothesis by giving the relative order of the anisotropy: $R_\parallel > R_\perp$. The sizes measured in ordinary solvent (toluene) show a concentration effects on the global size, but not on the magnitude of anisotropy. This anisotropy seems to be independent of the spacer value for $3 \leq n \leq 6$. These measurements give a correlation between the change in the viscosity behavior and the overlap concentration c^* deduced from the R_G value in toluene. These present results may be qualitatively interpreted in the framework of a recent model by Warner et al.[33] The basic feature deduced is that one cannot expect an extreme, extended prolate or flattened oblate limit for flexible backbones. This study also suggests that the prolate anisotropic form could be a property of nematic solutions compared to the melt case. This can be experimentally verified by using PMA systems, for example, in lmw solvents. It would be interesting to perform similar measurements on longer chains with different hard-core nematic formulae to check the importance of these factors. This could help to determine if there is a clear dependence of the anisotropy, both sign and magnitude, on the chain length. Measurements using partial grafting of side groups could provide more experimental evidence for the model of Warner et al.

Acknowledgment. We are grateful to H. Finkelmann (West Germany) who provided the materials we used and for the close cooperation of M. Veyssie, C. Casagrande, and M. A. Guedeau. We benefited from fruitful and constructive discussions with M. Veyssie, F. Brochard, J. Prost, M. Kleman, F. Moussa, M. Warner, and P. Fabre.

References and Notes

(1) Proceedings of the International Conference on Liquid Crystal Polymers; July 1987, Bordeaux, France. *Mol. Cryst. Liq. Cryst.* **1987**, *153*, Part A; **1988** *155*, Part B.
(2) *Advances in Polymer Science*; Springer-Verlag: New York, 1984; Vol. 60/61, Liquid Crystal Polymers II/IV.
(3) Keller, P. *Macromolecules* **1984**, *17*, 2937; *Makromol. Chem., Rapid. Commun.* **1985**, *6*, 707.
(4) (a) Casagrande, C.; Veyssie, M.; Finkelmann, H. *J. Phys., Lett.* **1981**, *43*, L.671. (b) Casagrande, C.; Veyssie, M.; Nobler, C. *Phys. Rev. Lett.* **1987**, *58*, 2079. (c) Sigaud, G.; Achard, M. F.; Hardouin, F.; Mauzac, M.; Richard, H.; Gasparoux, H. *Macromolecules* **1987**, *20*, 578. (d) Fabre, P.; Casagrande, C.; Veyssie, M.; Finkelmann, H. *Phys. Rev. Lett.* **1984**, *53*, 993.
(5) Brochard, F.; Jouffroy, J.; Levinson, P. *J. Phys.* (*Les Ulis, Fr.*) **1984**, *45*, 1125.
(6) de Gennes, P.-G. In *Polymer Liquid Crystals*; Ciferi, A., Krigbaum, W. R., Meyer, R. B., Eds.; Academic Press: New York, 1982; Chapter 5.
(7) Vasilenko, S. V.; Shibaev, V. P.; Khokhlov, A. *Makromol. Chem.* **1985**, *186*, 1961.
(8) Kirste, R. G.; Ohm, H. G. *Makromol. Chem., Rapid. Commun.* **1985**, *6*, 179.
(9) Keller, P.; Carvalho, B.; Cotton, J. P.; Lambert, M.; Moussa, F.; Pepy, G. *J. Phys., Lett.* **1985**, *46*, L.1065.
(10) Moussa, F.; Cotton, J. P.; Hardouin, F.; Keller, P.; Lambert, M.; Pepy, G. *J. Phys.* (*Les Ulis*) **1987**, *48*, 1079.

(11) Kostromin, S. G.; Kunchenko, A. B.; Ostanevich, V. M.; Svetogorsky, D. A.; Shibaev, V. P., to be published.
(12) (a) Basu, S.; Ramos, A.; Sutherland, H. H. *Mol. Cryst. Liq. Cryst.* **1986**, *132*, 29. (b) Davidson, P.; Keller, P.; Levelut, A. M. *J. Phys. (Les Ulis, Fr)* **1985**, *46*, 939.
(13) (a) Boeffel, C.; Spiess, H. W.; Hisgen, B.; Ringsdorf, H.; Ohm, H. G.; Kirste, R. G. *Makromol. Chem., Rapid. Commun.* **1986**, *7*, 777. (b) Spiess, H. W. *Colloid. Polym. Sci.* **1983**, *261*, 193. Boeffel, C.; Spiess, H. W. *Macromolecules* **1988**, *21*, 1626.
(14) Attard, G. S.; Williams, G.; Gray, G. W.; Lacey, D.; Gemmel, P. A. *Polymer* **1986**, *27*, 185.
(15) Coles, H. J. *Faraday Discuss. Chem. Soc.* **1985**, *79*, 10 and references therein.
(16) Mazelet, G.; Kleman, M. *Polymer* **1986**, *27*, 714.
(17) Ghanem, A.; Noel, C. *Mol. Cryst. Liq. Cryst.* **1988**, *155*, 447.
(18) Mattoussi, H. Ph.D. Thesis, Paris VI, France, 1987.
(19) Mattoussi, H.; Casagrande, C.; Veyssie, M.; Guedeau, M. A.; Finkelmann, H. *Mol. Cryst. Liq. Cryst.* **1987**, *144*, 211.
(20) Brochard, F. *J. Polym. Sci., Polym. Phys. Ed.* **1979**, *17*, 1367.
(21) Fabre, P. Ph.D. Thesis, Paris XI, France, 1986.
(22) Mattoussi, H.; Ober, R.; Veyssie, M.; Finkelmann, H. *Europhys. Lett.* **1986**, *2*, 233.
(23) Wang, X. J.; Warner, M. *J. Phys. A: Math. Gen.* **1987**, *20*, 713.
(24) Guinier, A. Theorie et Technique de la Radiocrystallographie, Dunod Ed, Paris, 1964.
(25) (a) Zimm, B. H. *J. Chem. Phys.* **1948**, *16*, 1093. (b) Flory, P. J.; Bueche, A. M. *J. Polym. Sci.* **1958**, *27*, 219.
(26) (a) Dubault, A. Ph.D. Thesis, Paris VI, France, 1981. (b) Dubault, A.; Ober, R.; Veyssie, M. Cabane, B., *J. Phys. (Les Ulis, Fr.)* **1985**, *46*, 1227.
(27) (a) Higgins, J. S.; Dodgson, K.; Semleyn, J. A. *Polymer* **1979**, *20*, 554. (b) Duran, H.; Strazielle, C. *Macromolecules* **1987**, *20*, 2853.
(28) Flory, P. J. *Principle of Polymer Chemistry*; Cornell University Press: Ithaca, NY, 1953.
(29) *Small Angle X-ray Scattering*; Glatter and Kratky, Eds.; Academic Press: London, 1982.
(30) Rawiso, M.; Duplessix, R.; Picot, C. *Macromolecules* **1987**, *20*, 630.
(31) Reference 29, p 427.
(32) Finkelmann, H.; Wendorff, H. J. *Polymer Liquid Crystals*; Blumstein, A., Ed.; Plenum Press: New York, 1985; p 295.
(33) (a) Warner, M.; Gunn, J. F.; Baumgartner, A. B. *J. Phys. A: Math. Gen.* **1985**, *18*, 3007. (b) Wang, X. J.; Warner, M. *J. Phys. A: Math Gen.* **1986**, *19*, 2215. (c) Renz, W. *Mol. Cryst. Liq. Cryst.* **1988**, *155*, 549.
(34) de Gennes, P. G. *The Physics of Liquid Crystals*; Oxford University Press: Oxford, 1974.
(35) Berne, B. J.; Pecora, R. *Dynamic Light Scattering with Applications to Chemistry, Biology and Physics*; Wiley-Interscience: New York, 1976.
(36) It is worthwhile mentioning that the absence of point collimation detection at the PSPE counter affects neither the $R_{\parallel}$ and $R_{\perp}$ values nor the ratio of anisotropy $R_{\parallel}/R_{\perp}$. In fact we have checked that the integration of the scattered beam over the detector window height has no effect on $R_{\parallel,\perp}$ for the range of q values examined.[18] A very recent theoretical treatment of small-angle scattering data from uniaxial systems showed the same results: Saraf, R. F. *Macromolecules* **1989**, *22*, 675.
(37) The compensation does not imply that the PMS chain behaves like in the same way as a PDMS with the same molecular weight ($M \approx 34\,000$). In fact an ordinary chain with that value of M will give a higher value for R_G, with or without considering the local rigidity (statistical unit larger than the monomer unit), for PMS component.
(38) The case studied by Dubault et al.[26] could also be considered in the framework of the previous general expression (eq 16), with $\phi = v_f \equiv 0$ and $S_B \simeq S_A$. W will be less than 0 in this case.

A Molecular Model for Cooperative Local Motions in Amorphous Polymers

Keiichiro Adachi

Department of Macromolecular Science, Faculty of Science, Osaka University, Toyonaka, Osaka 560, Japan. *Received April 25, 1989; Revised Manuscript Received September 8, 1989*

ABSTRACT: A simple molecular model has been proposed for rotational motions of simple molecules in liquids and for local segmental motions in condensed polymer systems. In order to describe the behavior of cooperative segmental motions, we consider a model in which gears are rotating synchronously. The gear model predicts that the number of cooperatively moving segments increases with decreasing temperature and diverges at a critical temperature, T_0. Thus the relaxation time also diverges at T_0 as given empirically by the Vogel equation. This model as well explains the nonexponential correlation function given by the Kohlrausch-Williams-Watts equation and the diluent effect on the relaxation time.

Introduction

The primary relaxation process in amorphous polymers has been investigated by many authors by means of dielectric, mechanical, and other methods.[1] Although phenomenological features of the primary process have been well established, its molecular mechanism has not been explained theoretically.

A most familiar theory for mobility of polymer segments is the free-volume theory first proposed empirically by Doolittle.[2] This theory has been used successfully in an explanation of varieties of dynamic properties of amorphous polymers such as the temperature dependence of viscosity and relaxation time or shift factor.[3,4] However, the free-volume theory is phenomenological and does not provide us with a detailed molecular picture for the segmental motions.

Molecular theories based on a crankshaft model have been developed by Monnerie and his co-workers[5,6] and several other authors.[7-10] An approach based on an Ising model has also been studied theoretically by Budimir and Skinner.[11] In these models diffusion of a local conformation of a polymer chain has been described to express the correlation function of orientation of the segments. However, the effects of intermolecular interactions, which

0024-9297/90/2223-1816$02.50/0